Desalination and Water Treatment
www.deswater.com
doi: 10.5004/dwt.2019.24313

162 (2019) 331–340
September

Adsorption and kinetic studies of the removal of ciprofloxacin from aqueous solutions by diatomaceous earth

José A. García-Alonso[a], Belkis C. Sulbarán-Rangel[a], Erick R. Bandala[b], Jorge del Real-Olvera[c,*]

[a]*Department of Basic and Applied Science and Engineering, University of Guadalajara, Nuevo Periferico 555, Jalisco, Mexico, emails: alfredo.ga93@outlook.es (J.A. García-Alonso), sulbaranbelkis7@gmail.com (B.C. Sulbarán-Rangel)*
[b]*Division of Hydrologic Sciences, Desert Research Institute, 755 E. Flamingo Road, 89119-7363 Las Vegas, NV, United States, email: Erick.Bandala@dri.edu (E.R. Bandala)*
[c]*Environmental Technology, Center of Research and Assistance in Technology and Design of the State of Jalisco, Normalistas 800, Guadalajara, Jalisco, Mexico, Tel. +52-333-345-5200 Ext. 2129; email: jdelreal@ciatej.mx (J. del Real-Olvera)*

Received 5 December 2018; Accepted 20 April 2019

ABSTRACT

Pharmaceutical derivatives have been reported to affect several water bodies around the world. Therefore, developing treatments that remove them from the environment is a significant need. The main goal of this work was to use powdered diatomaceous earth (DE) as a low-cost natural adsorbent for ciprofloxacin (CIP) in aqueous solutions, employing synthetic CIP solutions of pure water and treated domestic wastewater. The influences of adsorption time, initial pH, CIP concentration, and DE dosage were evaluated after DE structure characterization using Fourier transform infrared spectroscopy, scanning electron microscopy, transmission electron microscopy, and X-ray diffraction. Diatomaceous earth was shown to have significant capabilities to remove CIP in aqueous phase, achieving pollutant equilibrium adsorption in 24 h. The best CIP removal efficiency was 97% (19.4 mg L^{-1}) using 2 g of DE, 20 mg L^{-1} of CIP, and pH = 2.0. The experimental results were fitted using second-order rate kinetics, with rate constant values in the $0.0077 \leq k_2$ (g mg^{-1} h^{-1}) ≤ 0.1984 range and correlation coefficients above 0.95. The adsorption results were fitted to the Freundlich and Langmuir isotherm equations and isotherm constants were estimated. The maximum adsorption capacity was assessed to be 105.1 mg CIP g^{-1} DE, suggesting good affinity between the pharmaceutical drug and the adsorbent.

Keywords: Ciprofloxacin; Adsorption; Diatomaceous earth; Wastewater; Biomaterial

1. Introduction

In recent years, a significant number of pharmaceutical derivatives and personal care products have been found in surface water, groundwater, and wastewater [1]. These products exhibit low biodegradability and tend to accumulate in aquatic systems [2]. The first studies referring to the quantification of pharmaceuticals in natural waters appeared in the 1980s, which identified salicylic acid and anticancer products in various aquatic environments [3–5]. Since then, antibiotics have been identified to be among the most frequently detected pharmaceuticals in the environment, and they can cause various adverse effects for people and ecosystems [6]. Therefore, there is a significant need to research cost-effective and feasible alternatives to eliminate these products from the environment [7].

Ciprofloxacin (CIP) is a quinolone antibacterial agent classified as second-generation fluoroquinolone with broad-spectrum action that is often used to treat human and

* Corresponding author.

animal bacterial infections [8,9]. The presence of CIP or any antibacterial derivative in wastewater and surface water is considered a significant environmental risk, even at very low concentrations, because these products can increase the antibiotic resistance of pathogenic bacteria and generate modifications in the biological balance of aquatic ecosystems [9]. Several studies have been carried out to remove CIP from aqueous solutions. More recent methods reported for CIP removal in aqueous phase include microalgae intake [10]; photocatalytic degradation [11,12]; adsorption in activated carbon [13], electrocoagulation [14,15], montmorillonites [16–18], or zeolites [19].

Diatomaceous earth (DE) is a nonmetallic clay mineral that comes from sedimentary rocks and has its origin in the prehistoric age, which is mainly formed by the fossilized cell walls (frustules) of microscopic aquatic plants called diatoms. When diatoms die, the silicates they absorbed from the environment sink to the bottom of the water bodies and form thick sedimentary silicate deposits. Diatomaceous earth is composed of fine and porous aggregates with variable texture and it can have lacustrine or marine origin depending on its location [20]. These large deposits of clay minerals have significant economic potential once they demonstrate sufficient thickness and material quality. Diatomaceous earth is particularly significant on an industrial level because its variety of geometric shapes and mechanical properties (e.g., low density, high surface area and porosity, adsorption capacity, and low thermal conductivity and chemical reactivity) [20–22] as a filter medium can be used to purify a wide variety of liquids generated during industrial processes [22]. Natural (raw) or modified (thermally or chemically treated) DE has been used to adsorb different pollutants and/or remove contaminants from synthetic and real wastewater. Representative studies include the adsorption of heavy metals [23–27], textile dyes [28], pesticides [29], and bisphenol-A [30]. However, only a few studies have used DE for the adsorption of pharmaceutical derivatives. The most recent studies used the mineral sorbent of diatomite to adsorb triclosan [31], tylosin [32], diclofenac sodium [21,33], and tetracycline [34].

The goal of this study was to assess the feasibility of using DE without previous treatment as a low-cost natural adsorbent to remove ciprofloxacin (CIP) in aqueous solutions, employing two synthetic CIP effluents: pure water and treated domestic wastewater to identify the influence of CIP concentration, initial pH, adsorption time, and DE dose to better understand the adsorption processes.

2. Materials and methods

2.1. Diatomaceous earth source and preparation

In this study, the raw diatomaceous earth (DE, $SiO_2 \cdot nH_2O$) was obtained from a deposit of clay mineral situated in Jalisco, Mexico (20° 18′ 54.50″ N; 103° 36′ 42.57″ W). The DE sample (1 kg) was collected from 20 different points within the deposit. The raw material was pulverized using a sphere mill, passed through metal sieves from 150 to 700 μm, and the fraction of particles between 450 and 600 μm was used for the adsorption experiments. The powdered DE was washed several times with deionized water to remove soluble impurities, dried for 8 h, stored in closed containers, and placed in a cold room (4°C) until use, as suggested in the literature [35].

The chemical characterization of DE was performed using Fourier transform infrared (FT-IR) spectroscopy. Spectra were obtained with a Spectrum GX spectrometer (PerkinElmer, Waltham, MA, USA) carried out in the 4,000 to 550 cm^{-1} range using a resolution of 4 cm^{-1} and a powder X-ray diffractometer (D500 Model Kristallographie Siemens, Washington D.C., USA) with a Cu Ka radiation (0.1542 nm wavelength). High-angle X-ray diffraction (XRD) data were accumulated from 5° to 40° at 0.02° increments and 1 min count times. Diatomaceous earth images were obtained using transmission electron microscopy (TEM) (JEOL Mag: 15Kx at 200 kV). For TEM observation, DE samples were suspended in ethanol and sonicated for 10 min, and then the suspension was deposited drop-wise on a copper grid coated with carbon conductive tape film and dried at room temperature until the ethanol was evaporated. The DE morphology was also assessed by scanning electron microscopy (SEM; TESCAN, Brno-Kohoutovice, Czech Republic). The images were analyzed using the ImageJ 1.45 software to evaluate the porosity of the material. Specific surface area of sorbent (BET area) was determined using a Quantachrome sorptometer (Nova 2200e). Diatomaceous earth particle zeta-potentials were determined using a Litesizer 500 instrument, and the results reported as the arithmetic mean and standard deviation of three analyses. The solids were initially disseminated in an electrolyte buffer solution (pH 3) of boric acid and potassium chloride, other buffer of sodium and potassium phosphate was used for pH 6, and finally a buffer solution of potassium chloride and sodium hydroxide (NaOH) was used for pH 9. A more complete chemical characterization of the material was previously published by our research group [36].

2.2. Synthetic pure water solution of ciprofloxacin

Ciprofloxacin (CIP; $C_{17}H_{18}FN_3O_3$, mw 331.34 g mol^{-1}, water solubility at 20°C, 30 g L^{-1}) was obtained from Sigma-Aldrich (Germany) and its structural formula is shown in Fig. 1a, along with CIP speciation as a function of pH (Fig. 1b) [3,11].

For quality control, all the materials used in the laboratory for this study were new and carefully washed with a solution of Extran® 02 (5%) (Merck, Germany), nitric acid (5%) (Fermont, 64% to 66% purity), acetone (Jalmek, analytical grade), and deionized water before each experiment. In addition to the above, an ultrasonic bath (Branson 5510) was used to ensure thorough cleaning of the material and to prevent the interference of another contaminant.

A stock solution of CIP at an initial concentration of 1,000 mg L^{-1} in ultrapure water was prepared each week to avoid degradation. To dissolve the CIP in water, the pH was lowered to 3 with 0.1 M HCl (Sigma-Aldrich) following the procedure recommended by the manufacturer (Sigma-Aldrich), in the product's safety data sheet [37]. The stock solution was then stored in a cold room at 0°C–4°C in the dark. The initial pH of the different CIP working solutions was modified with 0.1 M HCl or NaOH to assess the influence of the initial pH (2–10) on the adsorption efficiency of DE. Also, working solutions with diverse concentrations

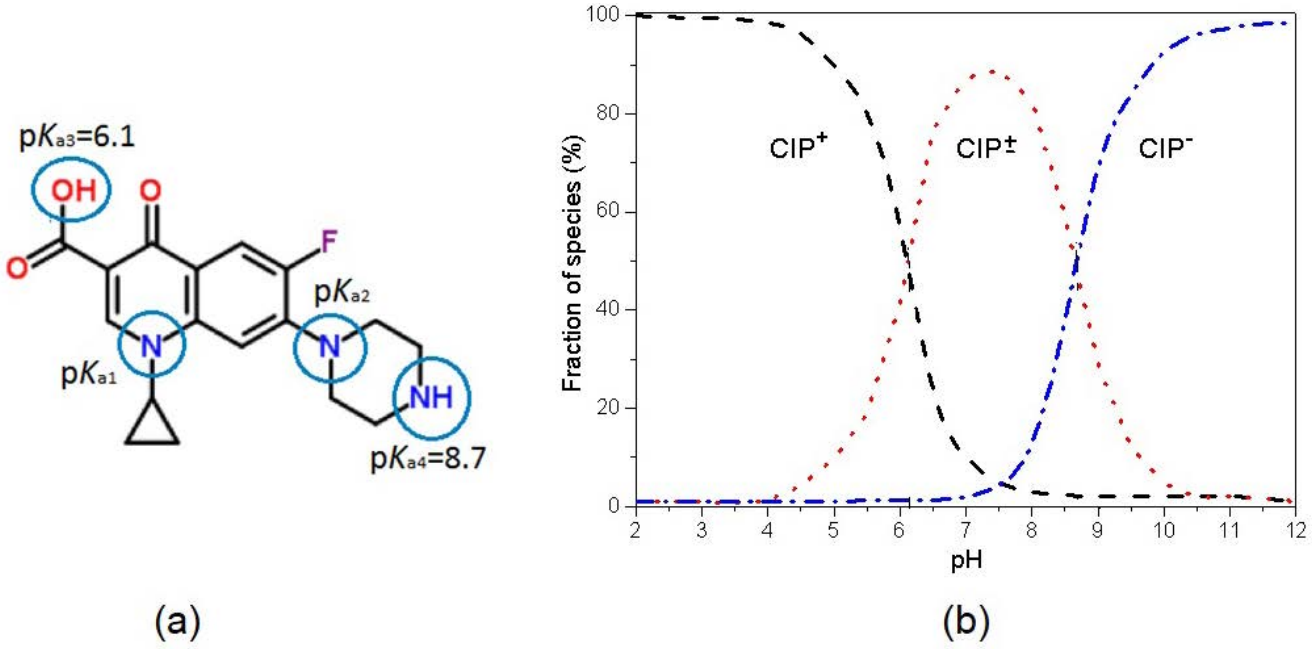

Fig. 1. (a) Ciprofloxacin structural formula and (b) speciation as a function of solution pH [3,11].

of CIP (5–50 mg L^{-1}) were also enhanced to investigate the influence of initial CIP concentration on the adsorption efficiency. All the chemical reagents used were of analytical grade.

2.3. Synthetic treated domestic wastewater with ciprofloxacin

To verify and validate the efficiency of the adsorption process of CIP onto DE, synthetic solutions were prepared employing treated domestic wastewater and ciprofloxacin. The treated wastewater was obtained from a domestic wastewater treatment plant situated in Jalisco, Mexico (20° 43′ 24.8″ N; 103° 23′ 52.2″ W). The wastewater treatment process consisted of fine screening, followed by settling, and anaerobic treatment. The effluent was characterized for chemical oxygen demand (COD), total nitrogen, total phosphorus, nitrates, and ammonia concentration and spiked with the same amount of CIP as described in section 2.2.

In all cases, the ciprofloxacin concentration was monitored using a UV-visible spectrophotometer trademark Hach (Model DR 5000) at 271 nm by preparing a calibration curve ranging from 1 to 70 mg L^{-1} for CIP at a neutral pH, as is suggested in the literature [38–40].

2.4. Adsorption and kinetic studies

Adsorption trials were carried out in batch mode with controlled temperature (25°C ± 3°C), using 2,000 mL beakers and a heating plate with a magnetic stirrer (Vante, MS7–H550). In all cases, the aqueous solutions were stirred for homogenization. The CIP concentration in the system was monitored for 48 h, and it reached adsorption equilibrium after 24 h. The adsorption process was followed through time: one 10 mL sample was taken every 10 min during the first 3 h; after the first 3 h, samples were taken every hour until completing 12 h; and the final samples were taken after 24 and 48 h. All samples were filtrated using 0.45 μm membrane filters to avoid the presence of adsorbent particles.

The experimental conditions tested during the study included initial pH (2–10), CIP concentration in working solutions (5–50 mg L^{-1}), and the dosage of DE (0.5–3.0 g L^{-1}), this last condition agrees with literature for the application of DE in the adsorption of emerging contaminants [31–34]. The adsorption capacity at equilibrium and at every time (t) was determined using Eqs. (1) and (2), respectively:

$$q_e\left(\text{mg g}^{-1}\right)=\frac{\left(C_i-C_e\right)V}{W} \tag{1}$$

$$q_t\left(\text{mg g}^{-1}\right)=\frac{(C_i-C_t)V}{W} \tag{2}$$

where q_e and q_t are the adsorption capacity in equilibrium (e) and at any time (t) of CIP (mg of CIP adsorbed/g of DE); C_i and C_e are the initial and equilibrium CIP concentrations (mg L^{-1}), respectively [9,18]; V is the volume (L); and W is the amount of DE powder (g). To estimate the capacity of adsorption at any time (q_t), it is necessary to change the equilibrium concentration (C_e) by the CIP concentration at any time (C_t), as shown in Eq. (2). Every experiment was performed in triplicate and the results corresponded to the average of experiments with 95% confidence in standard deviation. The statistical functions of Statgraphics Centurion XVI® (Statgraphics.Net, Madrid) were used for statistical analyses of experimental data.

Experimental results were fitted using the Freundlich and Langmuir isotherm equations to depict the equilibrium

relationships in all the tests made under several conditions of operation [9,18].

Eq. (3) was used to calculate CIP removal efficiency, for which C_i and C_t are the CIP initial and any time (h) concentrations (mg L^{-1}), respectively [23].

$$\text{Removal efficiency}(\%) = \frac{(C_i - C_t)}{C_i} \times 100 \quad (3)$$

3. Results

3.1. Chemical characteristics of adsorbent

The raw DE exhibited low specific surface area (BET = 29.14 ± 1.41 $m^2 g^{-1}$), but in the same order of magnitude as previous studies by other researchers for similar materials (32 $m^2 g^{-1}$) [31–32,35]. To assess the porosity of the adsorbent, SEM images were evaluated using the ImageJ software to quantify the pore diameter. Through this process, pore diameter was found to be in the 50–380 nm range, with an average diameter value of 190 ± 70 nm [36,41]. The zeta value of DE at all the pH values tested (pH = 3) was negative. The zeta potential of DE was −38.3 ± 0.4 mV at pH 9, −32.7 ± 0.3 mV at pH 6 and –25.9 ± 0.2 mV at pH 3.

A typical XRD spectrogram is presented in Fig. 2a and the data indicate that DE contains mainly silica (SiO_2) and small amounts of Fe_2O_3, Na_2O, Al_2O_3, and CaO. The XRD patterns of DE samples confirm the existence of feldspar, $Na(AlSi_3O_8)$ (29°, 23°, and 22°), quartz (SiO_2) (27°), and cristobalite (36° and 39°), which agrees with the literature [20,35]. The XRD diffraction suggested that the configuration of DE is poorly crystallized. The composition of the DE structure was confirmed by FT-IR, as shown in Fig. 2b. The signal at 3,400 cm^{-1} is identified as O–H stretching of physically adsorbed water and the signal at 1,630 cm^{-1} is characteristic of the H–O–H bending vibration of water. The representative components of DE are displayed in the bands at 1,020; 800; and 453 cm^{-1}. In this case, the siloxane (Si–O–Si) group is associated with the band at 1,020 cm^{-1}, whereas the band at 800 cm^{-1} is correlated to the quartz and free silica, and finally the band at 453 cm^{-1} is associated with the Si–O–Si and/or Si–O–Al [36].

The TEM image in Fig. 3a shows a heterogeneous distribution of arrays on frustules. The average frustule size was calculated as 10.13 μm, whereas the average frustule width was 2.84 μm. The TEM image has good agreement with the SEM image shown in Fig. 3b. From the SEM image, it was possible to determine that a great part of the DE has a circular form that was consistent with the *Discostella* species, which is reasonably in agreement with previous reports in the literature [42].

3.2. Adsorption kinetic process

The kinetic models more frequently reported in the literature were used to evaluate the adsorption mechanisms of the process. The adsorption kinetics data obtained for sorption of CIP over DE were fit to both the pseudo-second and pseudo-first-order models [9,13,16]. The integrated form of the Lagergren pseudo-first-order model is one of most widely used and it can be expressed with the limit conditions from $t = 0$ to $t = t$ and from $q = 0$ to $q = q_t$, which provides the following linear function:

$$\log(q_e - q_t) = \log q_e - \frac{k_1 t}{2.303} \quad (4)$$

where k_1 is the rate constant of the pseudo-first-order model (h^{-1}), whereas the capacity of adsorption in any time (q_t) is the quantity of CIP adsorbed during that time (t) (mg g^{-1}), and q_e is the CIP equilibrium adsorption capacity (mg g^{-1}).

For a pseudo-second-order kinetic mechanism, the linearized form considering the same boundary conditions (e.g., from $t = 0$ to $t = t$ and from $q = 0$ to $q = q_t$) is:

$$\frac{t}{q_t} = \frac{1}{k_2 q_e^2} + \frac{t}{q_e'} \quad (5)$$

where k_2 is the rate constant of the pseudo-second-order kinetics (g mg^{-1} h^{-1}), whereas q_t is the amount of CIP adsorbed at any time (t) (mg g^{-1}), and q_e is the equilibrium adsorption capacity (mg g^{-1}).

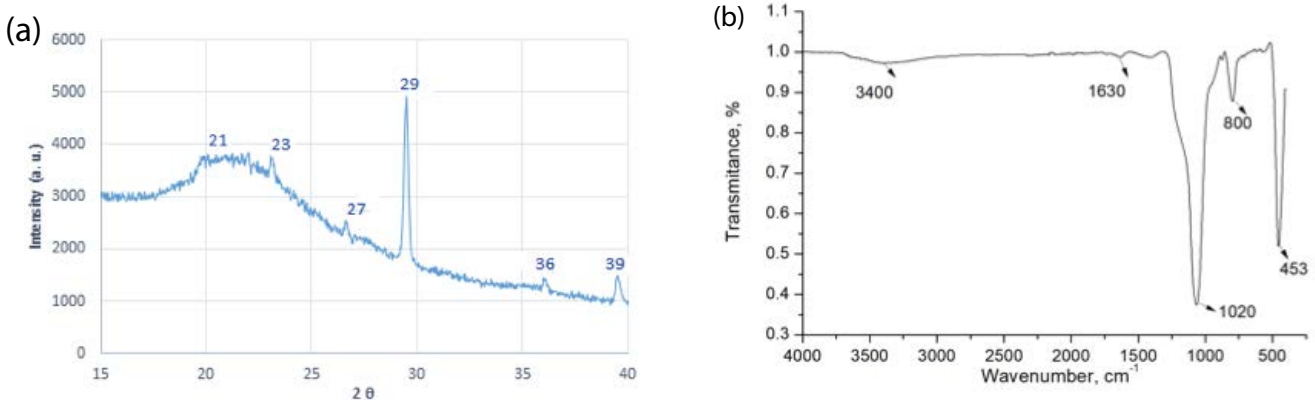

Fig. 2. Composition of structure of DE: (a) XRD spectrogram and (b) FT-IR spectra.

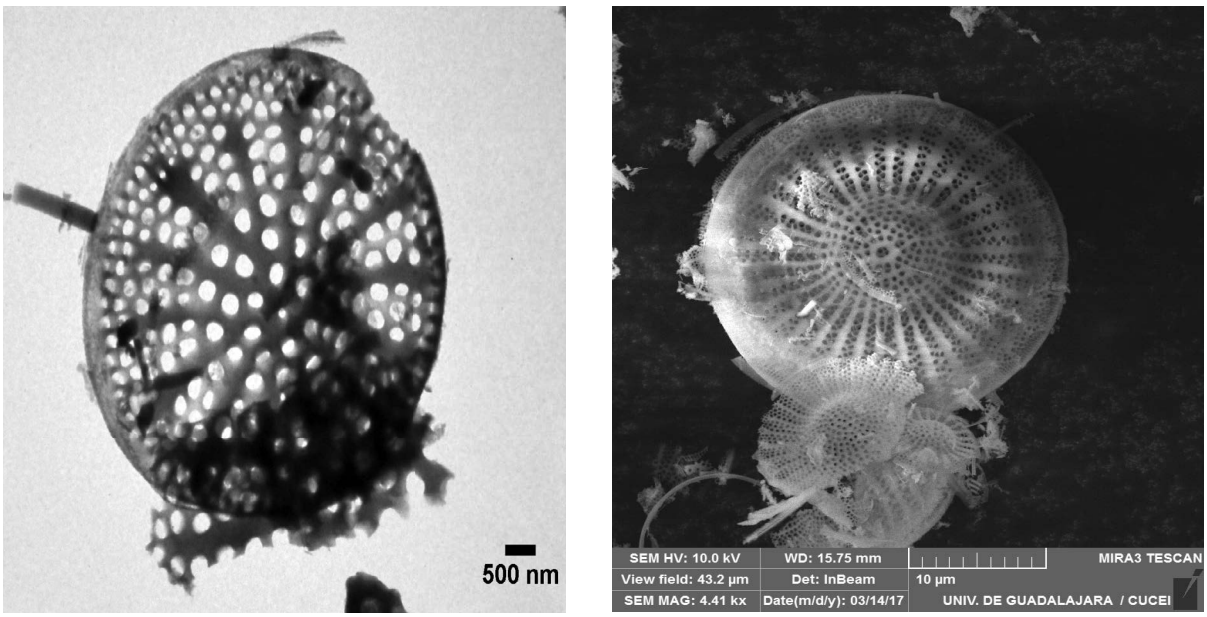

Fig. 3. Image of *Discostella* species: (a) TEM image and (b) SEM image.

The sorption of CIP onto DE was monitored for the synthetic pure water and treated domestic wastewater samples through to time at three different initial pH values, containing anionic (pH 9), zwitterionic (pH 6), and cationic (pH 3) species, as shown in Fig. 4. In both cases, the adsorption capacity in the process was examined for a contact time of 48 h in all experiments. However, the results showed that system required only of 24 h before it reached adsorption equilibrium. The first hours of the sorption process are the most important because the greatest adsorption capacity is reflected during this time. The results confirm that adsorption is very quick at low pH values, which indicates the involvement of cation species in the process. This trend is in agreement with similar systems reported by other researchers [31], which suggests that a contact time between 24 and 72 h is needed to reach adsorption equilibrium for triclosan over DE.

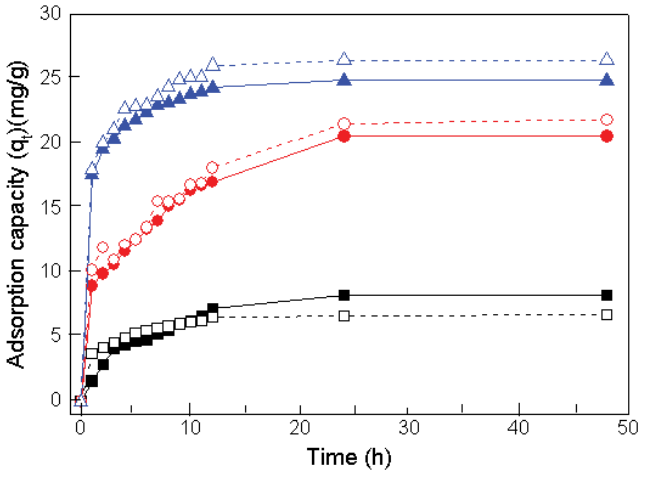

Fig. 4. Adsorption kinetic data for CIP on DE as a function of pH, using 1.5 g of DE and 30 mg L^{-1} of CIP with pH 3 ▲, pH 6 ●, and pH 9 ■ for synthetic pure water, and pH 3 △, pH 6 ○, and pH 9 □ for synthetic treated domestic wastewater.

The kinetic parameter values obtained using linear regressions for the two models proposed are summarized in Table 1 [3,8,16]. As shown, although correlation coefficients (R^2) in the regressions for both equations are greater than 0.80 for the entire range of pH values, the pseudo-second-order model better represents the kinetic behavior of the system, which is in agreement with the data obtained by other researchers [43]. In this study, the range obtained for the pseudo-second-order kinetic constant (k_2) was in the $0.007 \leq k_2$ (g mg^{-1} h^{-1}) ≤ 0.198 range with R^2 above 0.95, suggesting that the adsorption kinetic process was preferably regulated by chemisorption. A similar behavior was reported for CIP adsorption on montmorillonite with k_2 values in the $0.02 \leq k_2$ (g mg^{-1} h^{-1}) ≤ 0.17 range and $R^2 = 0.99$ for the same initial pH values [18].

3.3. Influence of initial pH on adsorption experiment

It is well recognized that the solubility of CIP is a function of pH, which is explained by the presence of different CIP chemical species at the different pH values in Fig. 1b. At low pH values, a highly soluble CIP^+ species occurs and its fraction value decreases as pH values move from 2.0 to 6.1, where the pK_{a3} constant value (carboxylic acid group) is located. For the pH range from 6.1 to 8.74 (pK_{a4}, nitrogen on piperazinyl ring), three different species are reported, with the $CIP^{\pm}$ zwitterion being the least soluble. Finally, as the pH value continues to increase to higher than 8.7, CIP becomes more soluble because of the appearance of the CIP^- species [12,15–17]. In agreement with the solubility of the different

Table 1
Pseudo-second and pseudo-first-order kinetics parameters with different pH values

		pH 3	pH 6	pH 9
Pseudo-first-order	q_e (mg g^{-1})	18.311	11.416	13.026
	k_1 (1/*h*)	0.2207	0.1746	0.1788
	R^2	0.9191	0.8371	0.9161
Pseudo-second-order	q_e (mg g^{-1})	25.498	21.251	12.225
	k_2 (g mg^{-1} h^{-1})	0.0343	0.0691	0.0336
	R^2	0.9966	0.9973	0.9723

species produced by CIP at diverse pH values, the influence of pH in solution on the removal of CIP using DE was assessed. Fig. 5 shows the removal efficiency of CIP on DE at different pH values.

The results show high CIP removal efficiency, independently of the effluent treated, at low pH, which decreases when pH values are close to 6, where the dissociation constant (pK_{a3} = 6.1) is located. This behavior can be described through the relationship between CIP total charge and the surface charge of DE. The zeta potential of DE was −38.3 ± 0.4 mV at pH 9, −32.7 ± 0.3 mV at pH 6 and –25.9 ± 0.2 mV at pH 3. When the system has a very basic pH (pH = 9), the DE surface shows a negative charge that is higher than when the solution has an intermediate pH (pH = 6) [35,36]. When the cationic CIP form (CIP^+) is present, the negative DE surface will perform a significant adsorption of the pollutant. These data are in agreement with the cation exchange adsorption mechanism of cationic CIP species for the natural cations present within the DE interlayer that has been suggested by other researchers [17].

The removal efficiency decreases significantly after the initial pH value reaches 8. This performance can be associated with the presence of the anionic CIP form (CIP^-), which can produce repulsive interactions with the DE negative surface [42]. For this study, only the main dissociation or ionization constants (pk_{a1} and pk_{a2}) are reported because at present there is no consensus about the value of these constants in acidic conditions. However, estimations can be made because pK_{a3} and pK_{a4} values have been reported as determining the relevant species of CIP under environmental conditions [17,18].

3.4. Effect of CIP concentration

Fig. 6 shows the removal efficiency of CIP on DE for different initial CIP concentration (5 to 50 mg L^{-1}) using pH = 3.0 and 2 g of DE. As expected, the highest removal efficiency was found when low initial CIP concentration was tested. However, removal efficiency was found to be higher than 90% for the entire range of initial CIP concentrations tested, which suggests that DE is a good adsorbent of the pollutant. Ciprofloxacin has been identified in surface water and wastewater at concentrations habitually <1 mg L^{-1} [16–18], whereas it ranges from 3 to 87 mg L^{-1} in hospital effluents [40] and was reported to be 31 mg L^{-1} for pharmaceutical industry effluents [43–45]. In the case of the synthetic treated wastewater used in this work, presence of COD as high as 77 mg L^{-1}, total nitrogen 69 mg L^{-1}, total phosphorous 22.6 mg L^{-1}, nitrates 0.005 mg L^{-1} and ammonia nitrogen 67.2 mg L^{-1} in the wastewater did not show any significant effect on the performance of the adsorbent. Based on Fig. 6, it is clear that DE is capable of removing concentrations orders

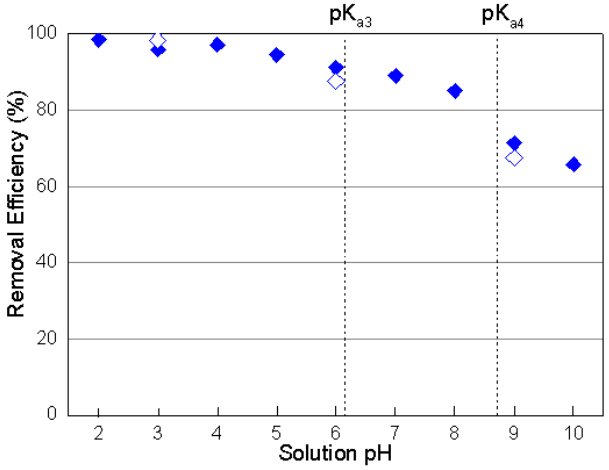

Fig. 5. Removal efficiency of CIP on DE at different pH values using 20 mg L^{-1} CIP and 2 g DE, for synthetic pure water (◆), and synthetic treated domestic wastewater (◇).

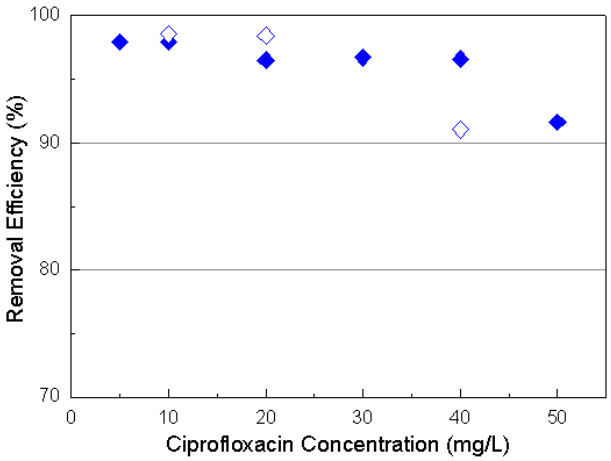

Fig. 6. Effect of the initial concentration of CIP on removal efficiency with pH 3 and 2 g DE, for synthetic pure water (◆), and synthetic treated domestic wastewater (◇).

of magnitude higher than that reported in the different effluents, and the presence of other wastewater components does not pose a threat in its application. Our results agree with other reports for CIP adsorption using different materials [9,14–15,17].

3.5. Effect of DE concentration

The effect of DE dosage on CIP adsorption in aqueous solutions is shown in Fig. 7. The removal efficiency was assessed as a function of the DE dose using 30 mg L^{-1} as initial CIP concentration at pH 3.0.

As shown, a relatively low DE dose (1 g L^{-1}) generated high removal efficiency of CIP after 24 h. Further increases in the DE dose (1–3 g L^{-1}) did not produce any significant difference in CIP adsorption capacity. The high CIP removal is probably because of the suggested strong affinity between the positively charged CIP molecules and the negatively charged DE surface, particularly when the system works at a low initial pH value. The performance of DE was very different at the lowest dose (e.g., 0.5 g L^{-1}), probably because under these conditions all the empty sites contained in the DE surface area were occupied by CIP molecules and there were still contaminant molecules in excess in the aqueous solution.

3.6. Estimation of adsorption capacity applying isotherms

Langmuir and Freundlich isotherm models were used to assess the relationships between the experimental data obtained under different operation condition and theoretical models. The results are shown in Table 2. These results confirm that the Langmuir equation fits the system fairly well because the R^2 value was better than 0.95, specifying that the constants (q_{max} and K_f) appropriately explain the sorption experimental results. From Table 2, q_{max} is DE maximum saturation, which was estimated to be 105.108 mg g^{-1}. This supports the results from Fig. 7, in which starting with 1.0 g, DE was able to almost completely remove CIP and no effect was noticed for further increase in the DE dose.

Table 2
Parameters of Freundlich and Langmuir isotherms for CIP uptake by DE powder

	Model			
	Langmuir		Freundlich	
	q_{max} (mg g^{-1})	K_L (L g^{-1})	n (dimensionless)	K_f (L g^{-1})
	105.108	1.49	5.586	0.479
R^2	0.9526		0.7092	

The Langmuir model describes monolayer adsorption on a set of adsorption sites with the same sorption energies independent of surface coverage and without interaction between adsorbed and incoming molecules [17]. Therefore, this is the most likely process occurring for CIP adsorption in DE because the Langmuir model best describes the experimental data.

Furthermore, the chart of C_e/q_e vs. C_e for the CIP in the aqueous solution (Fig. 8) was elaborated to verify the relationship between the experimental data and the results from the Langmuir model. Finally, Table 3 displays CIP adsorption capacity values using various adsorbents reported in the literature [45].

As is indicated in Table 3, different natural or synthetic materials have been reported in the literature to be efficient adsorbents in the elimination of CIP from aqueous solution. Of the materials analyzed, it is interesting to verify that the mineral clays exhibit different adsorption capacities (e.g., rectorite q_{max} = 135 mg g^{-1}, kaolinite q_{max} = 6.3 mg g^{-1}, and montmorillonite q_{max} = 400 mg g^{-1}) after different pre-treatments [45]. In this study, the raw DE used as adsorbent powder was only washed with deionized water to eliminate possible organic contaminants present in the surface of the material. The adsorption capacity shown by DE in the experiments (105.11 mg g^{-1}), despite the lack of chemical purification or physical treatment, suggesting its possible use as a viable alternative for removing CIP in contaminated effluents.

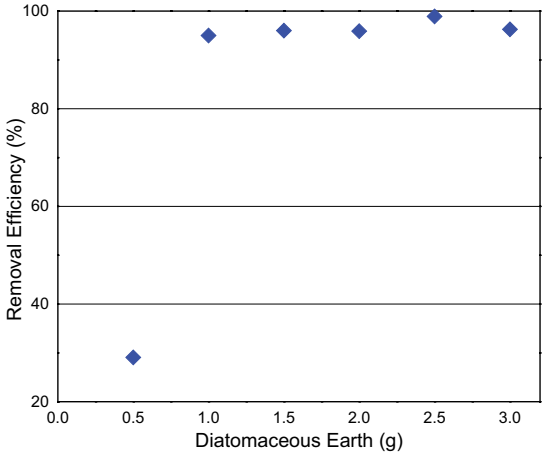

Fig. 7. Effect of DE concentration on the removal efficiency with pH 3 and 30 mg L^{-1} of CIP.

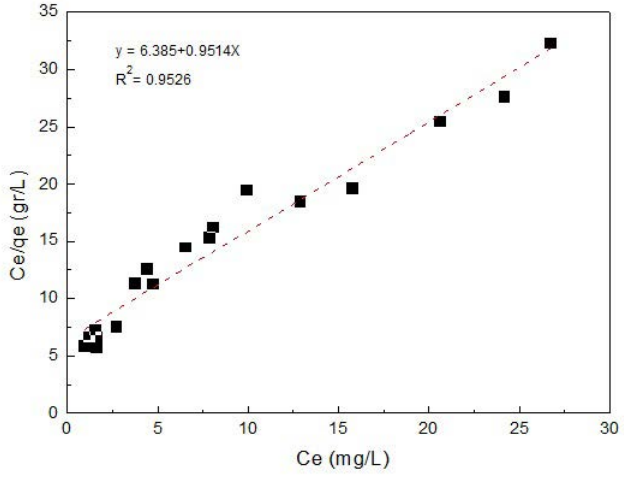

Fig. 8. Adjusted linearized Langmuir isotherm model (--) to the experimental data (■).

Table 3
Evaluation of CIP adsorption capacity with various adsorbents and DE [45]

Pollutant	Adsorbent	Temperature (°C)	pH	Adsorption capacity q_m (mg g^{-1})
CIP	Kaolinite	–	3.0–4.5	6.3
	Goethite	22	5	19.88
	Chemically prepared carbon	25	6	104.2
	Rectorite	–	4.0–5.5	135
	KMS-1	25	4	230.9
	Montmorillonite	–	3	400
	Activated carbon	25	6	434.8
	EDTA/β-CD	25	–	327.14
	KF	25	6.5	181.32
	Graphene oxide	25	5	379
	Fe_3O_4/C	25	7	98.28
	ZIF-8 derived carbon	25	6	416
	$CAMoS_4$·LDH	25	6	707.2
	DE[a]	25	3.0–9.0	105.108

[a]This study.

3.7. Proposed mechanism for adsorption

Fig. 9 shows a suggested mechanism of interaction between the raw DE powder and the ciprofloxacin in aqueous solutions, including the effect of initial pH value variations on adsorption capacity.

The analysis of the experimental data suggests that the mechanism implicated in the adsorption of CIP by DE is strongly related to pH value in aqueous solution. Three different pH ranges were identified: low pH value range (2–6), in which the cationic species CIP^+ are predominant; medium pH value range (7–8), in which three different species of CIP occur simultaneously in the system, with $CIP^{\pm}$ zwitterion being the least soluble; and high pH value range (9–12), in which the anionic species CIP^- is the dominant species. At low pH values, the predominant mechanism is charge neutralization, which is favored by the interaction between the positive charges of the CIP species and the negative charges on DE surface. The negatively charged functional groups generated when the adsorbent come into contact with water (SiO_2, Fe_2O_3, CaO, Na_2O) interact with the positive charged species of CIP. Surface charge neutralization generates flocs, which can easily be removed by settling. Another important observation of the behavior in this system is that the final value resulting from zeta potential after the treatment is the neutral charge (0.65 mV) [36].

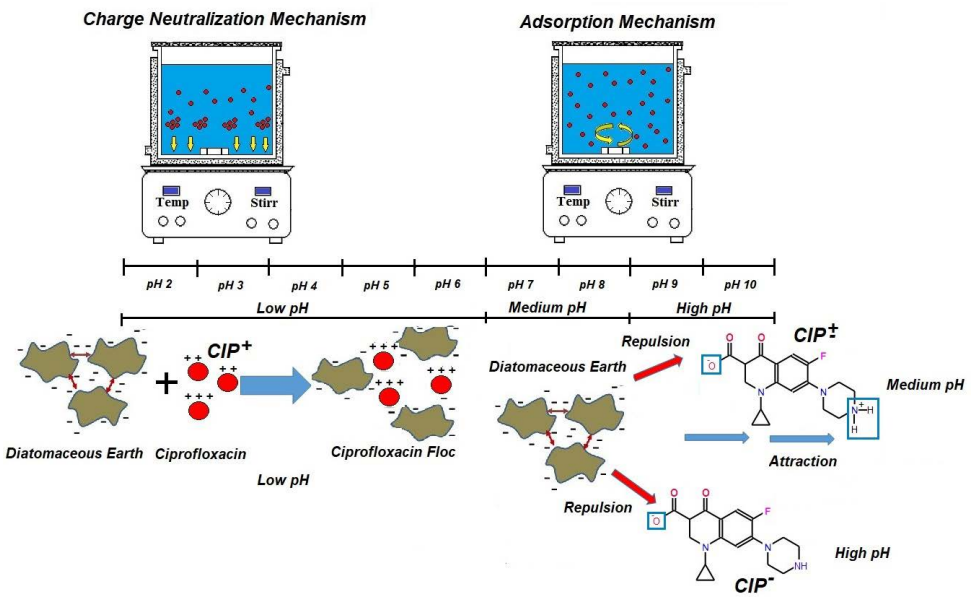

Fig. 9. Proposed mechanism for CIP uptake by DE powder at different pH values.

At medium pH values, CIP generates negatively and positively charged species that interact with the functional groups of DE ($FeOH_2^+$, $C–N^+$, N–H, $C=O^-$). The oxygen in the functional groups present in CIP, such as the carboxylic acids, will promote adsorption through hydrogen bonding mechanism, regardless of pH value [45]. Finally, at high pH values, only negatively charged CIP species are present to interact with the chemical species on DE surface with negative charge, this possibly causing electrostatic repulsion that leads to the observed reduction in removal efficiency [44].

4. Conclusions

In this study, CIP adsorption by a raw nonmetallic clay mineral was investigated. The following are the most significant findings:

- After using Langmuir and Freundlich models for fitting the experimental data, the linearized Langmuir isotherm model was found to be the best fit for the CIP/DE system. No significant differences were found for adsorption efficiency and isotherms measured at a low initial pH.
- The maximum adsorption capacity of DE toward CIP (q_{max}) was found to be 105.1 mg g^{-1}, which is comparable with several other natural materials. However, in this case, DE achieved interesting performance without any prior treatment, which suggests the importance of conducting further research into its application.
- As expected, initial pH, contact time, and initial CIP concentration were major parameters modulating CIP adsorption in DE, which defined the adsorption rate and pathway of the process.
- The pseudo-second-order kinetic model allowed the correct prediction of system trends and provided a basic understanding of the system that can be used in upscaling the adsorption process.
- No significant differences were found for the behavior of adsorption when were employed synthetic pure water and treated domestic wastewaters.
- All these result suggested good affinity between the pharmaceutical pollutants and the adsorbent.

Acknowledgments

The authors are grateful to National Council of Science and Technology (CONACyT) for their financial support (Grant No. 234633), as well as Ms. Nicole Damon (DRI) for the editorial review of this document.

References

[1] S.D. Richardson, S.Y. Kimura, Emerging environmental contaminants: challenges facing our next generation and potential engineering solutions, Environ. Technol. Innovation, 8 (2017) 40–56.
[2] M.B. Ahmed, J.L. Zhou, H.H. Ngo, W. Guo, Adsorptive removal of antibiotics from water and wastewater: progress and challenges, Sci. Total Environ., 532 (2015) 112–126.
[3] W.-T. Jiang, P.-H. Chang, Y.-S. Wang, Y. Tsai, J.-S. Jean, Z. Li, K. Krukowski, Removal of ciprofloxacin from water by birnessite, J. Hazard. Mater., 250–251 (2013) 362–369.
[4] A.M. Botero-Coy, D. Martínez-Pachón, C. Boix, R.J. Rincón, N. Castillo, L.P. Arias-Marín, L. Manrique-Losada, R. Torres-Palma, A. Moncayo-Lasso, F. Hernández, 'An investigation into the occurrence and removal of pharmaceuticals in Colombian wastewater', Sci. Total Environ., 642 (2018) 842–853.
[5] C.G. Daughton, Pharmaceuticals and the environment (PiE): evolution and impact of the published literature revealed by bibliometric analysis, Sci. Total Environ., 562 (2016) 391–426.
[6] M.-k. Liu, Y.-y. Liu, D.-d. Bao, G. Zhu, G.-h. Yang, J.-f. Geng, H.-t. Li, Effective removal of tetracycline antibiotics from water using hybrid carbon membranes, Sci. Rep., 7 (2017) 43717.
[7] K. Isaac-Olivé, A.E. Navarro-Frómeta, Detection of Pharmaceuticals in the Environment, L.M. Gómez-Oliván Ed., Ecopharmacovigilance: Multidisciplinary Approaches to Environmental Safety of Medicines, 1st ed., Springer International Publishing, Gewerbestrasse, Switzerland, 2017, pp. 1–18.
[8] M. Mezni, T. Saied, N. Horri, E. Srasra, Removal of enrofloxacin from aqueous solutions using illite and synthetic zeolite X, Surf. Eng. Appl. Electrochem., 53 (2017) 89–97.
[9] E.-S.I. El-Shafey, H. Al-Lawati, A.S. Al-Sumri, Ciprofloxacin adsorption from aqueous solution onto chemically prepared carbon from date palm leaflets, J. Environ. Sci., 24 (2012) 1579–1586.
[10] J.-Q. Xiong, M.B. Kurade, B.-H. Jeon, Can microalgae remove pharmaceutical contaminants from water?, Trends Biotechnol., 36 (2018) 30–44.
[11] M.A. Gharaghani, M. Malakootian, Photocatalytic degradation of the antibiotic ciprofloxacin by ZnO nanoparticles immobilized on a glass plate, Desal. Wat. Treat., 89 (2017) 304–314.
[12] A.R. Silva, P.M. Martins, S. Teixeira, S.A.C. Carabineiro, K. Kuehn, G. Cuniberti, M.M. Alves, S. Lanceros-Mendez, L. Pereira, Ciprofloxacin wastewater treated by UVA photocatalysis: contribution of irradiated TiO_2 and ZnO nanoparticles on the final toxicity as assessed by *Vibrio fischeri*, RSC Adv., 98 (2016) 95494–95505.
[13] M.J. Ahmed, Adsorption of quinolone, tetracycline, and penicillin antibiotics from aqueous solution using activated carbons: review, Environ. Toxicol. Pharmacol., 50 (2017) 1–10.
[14] M. Yoosefian, S. Ahmadzadeh, M. Aghasi, M. Dolatabadi, Optimization of electrocoagulation process for efficient removal of ciprofloxacin antibiotic using iron electrode; kinetic and isotherm studies of adsorption, J. Mol. Liq., 225 (2017) 544–553.
[15] S. Ahmadzadeh, A. Asadipour, M. Pournamdari, B. Behnam, H.R. Rahimi, M. Dolatabadi, Removal of ciprofloxacin from hospital wastewater using electrocoagulation technique by aluminum electrode: optimization and modelling through response surface methodology, Process Saf. Environ. Prot., 109 (2017) 538–547.
[16] C.-J. Wang, Z.H. Li, W.-T. Jiang. Adsorption of ciprofloxacin on 2:1 dioctahedral clay minerals, Appl. Clay Sci., 54 (2011) 723–728.
[17] C.J. Wang, Z.H. Li, W.T. Jiang, J.S. Jean, C.C. Chuan, Cation exchange interaction between antibiotic ciprofloxacin and montmorillonite, J. Hazard. Mater., 183 (2011) 309–314.
[18] M.E. Roca Jalil, M. Baschini, K. Sapag, Influence of pH and antibiotic solubility on the removal of ciprofloxacin from aqueous media using montmorillonite, Appl. Clay Sci., 114 (2015) 69–76.
[19] D. Zide, O. Fatoki, O. Oputu, B. Opeolu, S. Nelana, O. Olatunji, Zeolite 'adsorption' capacities in aqueous acidic media; the role of acid choice and quantification method on ciprofloxacin removal, Microporous Mesoporous Mater., 255 (2018) 226–241.
[20] Á. de Jesús Ruíz-Baltazar, Green composite based on silver nanoparticles supported on diatomaceous earth: kinetic adsorption models and antibacterial effect, J. Cluster Sci., 29 (2018) 509–519.
[21] J. Janićijević, D. Krajišnik, B. Čalija, V. Dobričić, A. Daković, J. Krstić, M. Marković, J. Milić, Inorganically modified diatomite as a potential prolonged-release drug carrier, Mater. Sci. Eng., C, 42 (2014) 412–420.
[22] M. Price, K. Walsh. Rocks and Minerals (Pocket Nature), 1st ed., Dorling Kinderley, 80 Strand, London WC2R 0RL, Great Britain, 2005, pp. 7–22.
[23] O.S. Bello, K.A. Adegoke, R.O. Oyewole, Insights into the adsorption of heavy metals from wastewater using diatomaceous earth, Sep. Purif. Technol., 49 (2014) 1787–1806.

[24] R.A. Crane, D.J. Sapsford, Towards "Precision Mining" of wastewater: selective recovery of Cu from acid mine drainage onto diatomite supported nanoscale zerovalent iron particles, Chemosphere, 202 (2018) 339–348.
[25] S.S. Salih, T.K. Ghosh, Adsorption of Zn(II) ions by chitosan coated diatomaceous earth, Int. J. Biol. Macromol., 106 (2018) 602–610.
[26] S.S. Salih, T.K. Ghosh, Highly efficient competitive removal of Pb(II) and Ni(II) by chitosan/diatomaceous earth composite, J. Environ. Chem. Eng., 6 (2018) 435–443.
[27] Y. Fu, Y. Huang, J. Hu, Z. Zhang, Preparation of chitosan/amine modified diatomite composites and adsorption properties of Hg(II) ions, Water Sci. Technol., 77 (2018) 1363–1371.
[28] A. Hethnawi, N.N. Nassar, A.D. Manasrah, G. Vitale, Polyethylenimine-functionalized pyroxene nanoparticles embedded on diatomite for adsorptive removal of dye from textile wastewater in a fixed-bed column, Chem. Eng. J., 320 (2017) 389–404.
[29] K. Agdi, A. Bouaid, A.M. Esteban, P.F. Hernando, A. Azmani, C. Camara, Removal of atrazine and four organophosphorus pesticides from environmental waters by diatomaceous earth-remediation method, J. Environ. Monit., 2 (2000) 420–423.
[30] W.T. Tsai, C.W. Lai, T.Y. Su. Adsorption of bisphenol-A from aqueous solution onto minerals and carbon adsorbents, J. Hazard. Mater., 134 (2006) 169–175.
[31] A.A. Sharipova, S.B. Aidarova, N. Ye Bekturganova, A. Tleuova, M. Kerimkulova, O. Yessimova, T. Kairaliyeva, O. Lygina, S. Lyubchik, R. Miller, Triclosan adsorption from model system by mineral sorbent diatomite, Colloids Surf., A, 532 (2017) 97–101.
[32] B.S. Stromer, B. Woodbury, C.F. Williams, Tylosin sorption to diatomaceous earth described by Langmuir isotherm and Freundlich isotherm models, Chemosphere, 193 (2018) 912–920.
[33] J. Janićijević, D. Krajišnik, B. Čalija, B.N. Vasiljević, V. Dobričić, A. Daković, M.D. Antonijević, J. Milić, Modified local diatomite as potential functional drug carrier—a model study for diclofenac sodium, Int. J. Pharm., 496 (2015) 466–474.
[34] X. Meng, Z. Liu, C. Deng, M. Zhu, D. Wang, K. Li, Y. Deng, M. Jiang, Microporous nano-MgO/diatomite ceramic membrane with high positive surface charge for tetracycline removal, J. Hazard. Mater., 320 (2016) 495–503.
[35] Z. Jian, P. Qingwei, N. Meihong, S. Haiqiang, L. Na, Kinetics and equilibrium studies from the methylene blue adsorption on diatomite treated with sodium hydroxide, Appl. Clay Sci., 83–84 (2013) 12–16.
[36] J.A. Garcia-Alonso, F. Zurita-Martinez, C.A. Guzmán-González, J. Del Real-Olvera, B.C. Sulbarán-Rangel, Nanostructured diatomite and its potential for the removal of an antibiotic from water, Bioinspired Biomimetic Nanobiomater., 1 (2018) 1–7.
[37] J.B. Parsa, T.M. Panah, F.N. Chianeh, Removal of ciprofloxacin from aqueous solution by a continuous flow electro-coagulation process, Korean J. Chem. Eng., 32 (2015) 1–9.
[38] X.V. Doorslaer, J. Dewulf, H.V. Langenhove, V. Demeester, Fluoroquinolone antibiotics: an emerging class of environmental micropollutants, Sci. Total Environ., 500–501 (2014) 250–269.
[39] J.A.L. Perini, A.L. Tonetti, C. Vidal, C.C. Montagner, R.F.P. Nogueira, Simultaneous degradation of ciprofloxacin, amoxicillin, sulfathiazole and sulfamethazine, and disinfection of hospital effluent after biological treatment via photo-Fenton process under ultraviolet germicidal irradiation, Appl. Catal., B, 224 (2018) 761–771.
[40] N. Carmosini, L.S. Lee, Ciprofloxacin sorption by dissolved organic carbon from reference and bio-waste materials, Chemosphere, 77 (2009) 813–820.
[41] A.S. Adeleye, J.R. Conway, K. Garner, Y. Huang, Y. Su, A.A. Keller. Engineered nanomaterials for water treatment and remediation: costs, benefits, and applicability, Chem. Eng. J., 286 (2016) 640–662.
[42] N. Inchaurrondo, J. Font, C.P. Ramos, P. Haure. Natural diatomites: efficient green catalyst for Fenton-like oxidation of Orange II, Appl. Catal., B, 181 (2016) 481–494.
[43] D.J. Larsson, C. de Pedro, N. Paxeus, Effluent from drug manufactures contains extremely high levels of pharmaceuticals, J. Hazard. Mater., 148 (2007) 751–755.
[44] S. Gummadi, D. Thota, S.V. Varri, P. Vaddi, P., V.L.N.S. Rao, Development and validation of UV spectroscopic methods for simultaneous estimation of Ciprofloxacin and Tinidazole in tablet formulation, Int. Curr. Pharm. J., 1 (2012) 317–321.
[45] K. Gupta, J.B. Huo, J.C.E. Yang, M.L. Fu, B. Yuan, Z. Chen, $(MoS_4)^{2-}$ intercalated $CAMoS_4$·LDH material for the efficient and facile sequestration of antibiotics from aqueous solution, Chem. Eng. J., 355 (2019) 637–649.